DOI 10.1007/s11182-020-01888-w

Russian Physics Journal, Vol. 62, No. 9, January, 2020 (Russian Original No. 9, September, 2019)

PHYSICS OF SEMICONDUCTORS AND DIELECTRICS

FEATURES OF RADIATION CHANGES IN ELECTRICAL PROPERTIES OF InAlN/GaN HEMTS

A. G. Afonin, V. N. Brudnyi, P. A. Brudnyi, and L. E. Velikovskii UDC 539.239: 537.312.5

The effect of the proton, electron, gamma - rays, and fast neutron irradiation on the parameters of InAlN/GaN *HEMT structures is analyzed. The features of initial electronic properties of the* InAlN *and* AlGaN *barrier layers with a change in their composition, as well as the change in these properties when exposed to high-energy radiation are considered with taking into account the compositional dependence of the charge neutrality level energy position in the energy spectrum of these barrier layers.*

Keywords: InAlN/GaN high electron mobility transistor, radiation resistance, charge neutrality level.

INTRODUCTION

High electron mobility transistors (HEMTs) are used in high frequency microwave communication systems. At the same time, HEMTs based on group III–N semiconductor compounds as compared to HEMTs based on cubic crystals of GaAs, InAs, etc. have high breakdown fields and a large output specific power. Such transistors also demonstrate the resistance to high energy radiation due to the strength of chemical bonds in AlN (11.52 eV), GaN (8.6 eV), and InN (7.72 eV). Thus, experimental estimates of the threshold atomic displacement energies (E_d) in GaN upon electron irradiation give the values of E_d(Ga) = (19 ± 2) eV [1], E_d(Ga) = 20.5 eV, and E_d(N) = 10.8. eV [2]. At the same time, the corresponding calculations using molecular dynamics methods give the values of E_d (Ga) = (22 ± 1) eV and E_d (N) = (25 ± 1) eV [3], E_d (Ga) = 39 eV, and E_d (N) = 17 eV [4]. In addition, high electron density in the region of two-dimensional electron gas (2DEG) in the nitrides-based HEMTs (~10^{13} cm^{-2}) and small thickness of their active region additionally provide them with radiation resistance higher than that of the corresponding structures based on cubic semiconductors. This makes nitride-based HEMTs suitable for use in on-board systems in near-Earth space. Currently, a significant amount of research is devoted to the problem of the influence of various types of radiation exposure on the parameters of AlGaN/GaN structures. Meanwhile, currently there are practically no similar systematic studies of more promising InAlN/GaN structures, which can provide an increase in the density of two-dimensional electrons by a factor of 2–3 in the conducting channel as compared to AlGaN/GaN HEMTs [5].

SPACE RADIATION FACTORS

Special features of the space environment include the presence of high-energy radiation, low temperatures, and space zero gravity. The factors of temperature and weightlessness can be taken into account when designing and testing HEMTs. The main factors of space exposure are the fluxes of charged particles – protons (~90%), alpha particles (~9%), nuclei of heavy elements (~1%), and electrons (~1%) involved in the formation of Van Allen radiation belts

National Research Tomsk State University, Tomsk, Russia, e-mail: aag@niipmm.tsu.ru; brudnyi@mail.tsu.ru; paul702600@gmail.com; velikovskiy@gmail.com. Translated from Izvestiya Vysshikh Uchebnykh Zavedenii, Fizika, No. 9, pp. 106–112, September, 2019. Original article submitted June 18, 2019.

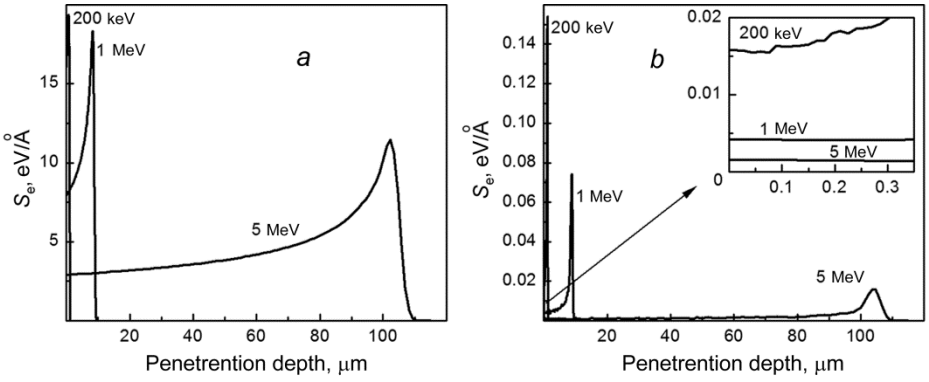

Fig. 1. Specific energy losses of protons with initial energies E = 0.2, 1, and 5 MeV on the electron S_e (*a*) and nuclear S_n (*b*) stopping in GaN.

around the Earth. The inner belt at altitudes from 1000 to 6000 km is mainly represented by protons with energies up to 600 MeV and a flux density up to 10^6 cm^{-2} s^{-1}. The outer belt at altitudes from 13 000 to 60 000 km contains mainly electrons with energies up to 10 MeV. The spatial and energy distributions of protons and electrons in the radiation belts are quite complex. It is common that main part of this distribution contains particles with low energy, and the density of particles rapidly decreases with the increase in their energy.

EFFECT OF RADIATION ON THE GALLIUM NITRIDE PROPERTIES

During bombardment, the charged particles lose their energy due to the nuclear (S_n) and electron (S_e) stopping in the irradiated target, while fast neutrons lose their energy due to the elastic scattering on atomic nuclei. In this case, nuclear stopping predominates at low particle energies, and electron stopping – at high energies of bombarding particles and light target atoms. Electron stopping of a particle causes ionization of the target atoms and, in case of HEMT, can lead to an increase in ionization currents, leakage currents, and charge density in the gate oxide of the structure. When nuclear stopping occurs, kinetic energy is transferred to the atom of the irradiated material, and when the transferred energy is greater than E_d, a radiation defect (RD) is formed in the target. In this case, the initially displaced atom of the semiconductor, which received an energy $E >> E_d$, in turn, is able to create a cascade of secondary, etc. atomic displacements. The particle energy loss, its average projected range R_p, the number and distribution of the displacement defects during the particle stopping in the target are calculated using SRIM/TRIM programs [6, 7]. The calculated values of the specific energy losses due to electron S_e and nuclear S_n stopping and the penetration depth of H^+-ions with E = 200 keV, 1 and 5 MeV in GaN are shown in Fig. 1 for E_d (Ga) = 39 eV and E_d (N) = 17 eV. Taking into account the small thickness of the active region of HEMT and the corresponding values of R_p = 1.12, 8.8, and 104 μm for protons of these energies, the greatest threat is represented by protons of low energies, whose value of R_p is comparable to the transistor active region thickness.

Accumulation of RDs in the lattice of a semiconductor causes a change in its electronic, optical, recombination, etc. properties. Moreover, the radiation modification of the electronic properties of a semiconductor is always a self-compensation process, as a result of which, at a high density of radiation defects, the initial Fermi level (F_0) of the material is shifted in the limiting position (F_{lim}) [8]. This limiting position is identical to the energy position of the charge neutrality level (CNL) of the semiconductor [8, 9]. Theoretical estimates of the CNL in AlN, GaN, and InN give values of about 3.5, 2.6, and 1.7 eV relative to the valence band top of these compounds, respectively [10, 11]. In this case, for the initial *n*-GaN samples, irradiation causes an increase in the material specific resistivity up to ~10^{10} Ω·cm (at 300 K) [12]. For the initial samples of *p*-GaN, there is a conversion of the conductivity type into *n*-type and the subsequent transition of the material to the high-resistance state of the ν-type conductivity, as in case of irradiation of an initial *n*-GaN. This suggests that upon irradiation, predominantly acceptor-type defects are introduced in *n*-GaN, and in

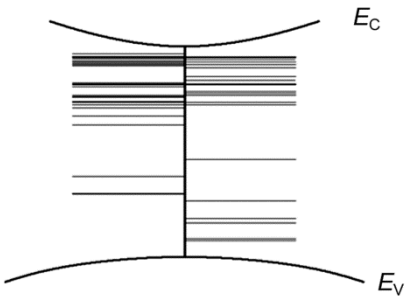

Fig. 2. Energy spectra of radiation defects in GaN irradiated by electrons (left) and protons (right) according to the data of [2, 13–32].

p-GaN, donor-type defects are introduced. The energy spectra of RDs in GaN were studied mainly by the DLTS and photocapitance spectroscopy methods. For the samples irradiated with electrons and protons, these data are summarized in Fig. 2 [2, 13–32]. It is worth noting that, despite a significant number of studies, today there is no general agreement on the distribution of energy levels of RDs in the GaN bandgap, the parameters of these traps, and their nature. For the majority of RIDs in GaN, these data are conjectural, and the point defects — vacancies, interstitial atoms, and antisite defects, as well as their complexes — are usually considered as main radiation defects [25, 28, 31]. The formation of radiation defects in the barrier and buffer layers affects the operability of HEMT structures.

EFFECT OF RADIATION ON THE PARAMETERS OF InAlN/GaN HEMT

It is known that InAlN layers grown on a GaN substrate can be biaxially compressed or stretched depending on the indium content. Of particular interest are lattice-matched (LM) structures with an In content of about 0.17, where a high degree of spontaneous polarization at the InAlN barrier is provided [33]. Most studies of the effect of radiation are devoted specifically to LM-structures grown by the MOCVD method on Al_2O_3 or SiC substrates. The studied structures had a thin (1–1.5 nm) spacer layer of semi-insulating AlN at the InAlN/GaN interface. Irradiation of InAlN/GaN structures with open contacts by protons, electrons, gamma quanta, and neutrons was carried out near room temperatures.

The bombardment of InAlN/GaN/SiC (x = 0.19 and 0.21) by protons (E = 3 MeV) in the dose range D = (1–4)·10^{14} cm^{-2} revealed a decrease in the drain saturation current (I_{DSS}) and a positive shift in the threshold voltage (V_{TH}) due to the formation of acceptor traps, as well as an increase in on-resistance (R_{ON}) of the structure due to a decrease in the mobility and density of electrons in the 2DEG-region. An increase in the gate leakage current and a decrease in the transconductance peak (g_m) of the current–voltage characteristic are noted. The pulsed measurements showed an increase in the current collapse due to the formation of traps between the gate and drain [34, 35].

Irradiation of LM-InAlN/GaN/SiC structure by protons (E = 5, 10, and 15 MeV, D = 5·10^{15} cm^{-2}) caused an increase of the layer (R_S) and contact (R_C) resistances, of the gate leakage current at the reverse bias, and of the subthreshold leakage in the static mode and a decrease of I_{DSS} and g_m. A ~10% degradation of the cut-off and maximum generation frequencies after irradiation by protons with E = 15 MeV was observed, and for protons with E = 5 MeV, these changes amounted to ~30% [36, 37].

Proton bombardment (E = 5 MeV, D = 2·10^{11}–2·10^{15} cm^{-2}) of LM-InAlN/GaN/SiC at highest doses caused a ~60% increase in R_S, a ~40% decrease in I_{DSS}, and a degradation of g_m due to the appearance of electron traps in the barrier layer and conducting channel, as well as a 6-fold increase in the reverse gate current and the degradation of the ON/OFF ratio by about 2 orders of magnitude, which correlates with an increase in the resistance of the conducting channel and an increase in the gate current [38, 39].

The bombardment of LM-InAlN/$Al_{0.04}$ $Ga_{0.95}N$/Al_2O_3 MOS with an Al_2O_3 gate oxide by protons (E = 5 MeV, D = 1·10^{13}–1·10^{15} cm^{-2}) at the maximum proton doses caused a ~ 9.7% increase in R_S at a catastrophic growth in R_C by

about 114% and a 54% increase in the transistor resistance (R_T) . These changes are presumably caused by the formation of defects at the metal - semiconductor interface during proton stopping in the thick (d = 200 nm) layer of the ohmic Ti/Al/Ni/Au contact with a slight defect formation in the thin active region of HEMT. An increase in the density of traps by about 4 times was found, which was proportional to the radiation dose [40].

According to the Raman thermography, proton irradiation (E = 340 keV, $D = 5 \cdot 10^{13}$ cm^{-2}) of InAlN/GaN initiated a ~10% increase in temperature of the channel due to an increase in its resistance and a ~15% decrease in its thermal conductivity. A ~42% increase in the breakdown voltage (V_{BR}) of the drain in the off-state and ~92% increase in the critical voltage (V_{CR}) were observed, which was associated with a ~50% decrease in the peak electric field at the gate edges due to the formation of negatively charged traps during irradiation [41].

The bombardment of LM-InAlN/GaN/Al_2O_3 by electrons (E = 10 MeV, $D = 2 \cdot 10^{15}$–$3.3 \cdot 10^{16}$ cm^{-2}) showed a ~50% decrease in the mobility of two-dimensional electrons for $D = 1.3 \cdot 10^{16}$ cm^{-2} and insignificant change in their density, despite the fact that no conductivity of the 2DEG region was observed for the highest electron dose $D = 3.3 \cdot 10^{16}$ cm^{-2}. Irradiation caused a positive shift in the capacitance–voltage characteristic of the transistor due to an increase in the concentration of acceptor traps in the barrier layer–interface region. At low electron doses, a negative shift of V_{TH} was observed, which is associated with the formation of shallow donor centers. With an increase in the radiation dose, a positive shift of V_{TH} occurs, as in cases of the proton and neutron irradiation [42].

Gamma irradiation with ^{60}Co (an absorbed dose up to 500 Mrad) caused noticeable changes in the LM-InAlN/GaN parameters at D> 200 Mrad. At D = 500 Mrad, a ~48% degradation of I_{DSS}, a ~13% positive shift of V_{TH}, and a ~17% decrease of the electron density in the 2DEG- region of the conducting channel were observed [43]. Gamma irradiation (E = 1.173 and 1.332 MeV, total ionization dose of 9.2 Mrad) of InAlN/GaN (x = 0.18) revealed a ~20% decrease in I_{DSS} and a ~20% increase in R_{ON} at the almost constant threshold voltage. Subsequent storage of irradiated structures at 300 K for 24 h and annealing at 100°C for 168 h made it possible to eliminate the observed changes in the heterostructure parameters [44, 45].

Irradiation of LM-InAlN/GaN with neutrons ($E \approx 2$ MeV) in the fluence range of $(1–3) \cdot 10^{15}$ cm^{-2} showed that the main effect of the neutron bombardment is a decrease in the mobility of two-dimensional electrons, a positive shift of V_{TH}, and a decrease in the density of 2DEG - electrons at the maximum neutron fluence [46].

It should be noted that a more significant sensitivity of the two-dimensional electrons mobility in InAlN/GaN HEMT to the effect of radiation at the initial stages of irradiation as compared with the electron density change was noted in other studies too [34, 41]. To explain this effect, one takes into account the deterioration of the transport characteristics of the conducting channel due to an increase in the two-dimensional electrons scattering at the InAlN/GaN interface caused by the increase in its isosurface roughness as a result of irradiation [47].

DISCUSSION OF EXPERIMENTAL DATA

It was found that the observed changes in the parameters of irradiated HEMT structures are caused by the radiation traps, mainly acceptor-type traps, which reduce the density of two-dimensional electrons and their mobility and increase the effect of electrons capture. In general, the results of studies of InAlN/GaN and AlGaN/GaN HEMTs showed their comparable stability under similar irradiation conditions. At the same time, a number of authors note an increased sensitivity of InAlN/GaN structures to irradiation compared to AlGaN/GaN or AlN/GaN structures, citing higher chemical bonding energies of latters [5, 40–42]. When assessing the radiation resistance of GaN-based HEMT structures, the carrier removal rates $-\Delta n/\Delta D$ (cm^{-1}) are usually compared. It should be noted that the parameter $\pm\Delta n(\Delta p)/\Delta D$ is primarily determined not by the threshold defect formation energy, but by the energy position of the limiting Fermi level F_{lim} in the irradiated semiconductor relative to the initial (before irradiation) position of the Fermi level (F_0), since $\pm\Delta n(\Delta p)/\Delta D \propto (F_0 - F_{lim})$. It is known that the undoped LM-InAlN layers have stable n-type conductivity with the concentration of free electrons $(1–8) \cdot 10^{18}$ cm^{-3}, presumably caused by the presence of residual donors based on oxygen and nitrogen vacancies [48–50]. Moreover, with an increase in the molar fraction of InN to ~0.4, the concentration of free electrons in these layers increases to approximately 10^{20} cm^{-3} [51]. At the same time, in AlGaN layers, an increase in the Al fraction from 0.3 to 0.5 leads to an increase in the specific resistivity of the layer from 0.18 Ω·cm to more than 10^5 Ω·cm, presumably due to the increase in the binding energy of residual donors [52]. In

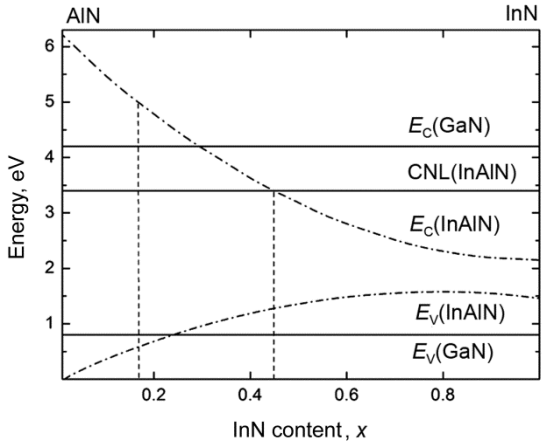

Fig. 3. Compositional dependence of the conduction band (E_C) and valence (E_C) edges of InAlN solid solution [54] and the energy position of the CNL level in InAlN.

this case, as a result of irradiation, the specific resistivity of AlGaN will increase for all compositions, which is caused by a shift of the Fermi level in the direction of CNL in this solution from ~E_C – 0.8 eV in GaN to ~E_C – 2.7 eV in AlN with a change in the composition of the solution within $0 \le x \le 1$ [10, 11]. At the same time, the nature of the change in the resistivity of InAlN layers upon exposure to radiation will be determined by the molar fraction of InN.

Figure 3 shows the compositional dependences of the bandgap and the conduction and valence band edges of the InAlN solid solution under the assumption that the corresponding bowing parameters b of these bands are determined by the InN content [53]. These data were obtained by analyzing the experimental results and numerical estimates taking into account local elastic strains arising from random local fluctuations in the composition of the InAlN solution. This means that the dependence of the bandgap and its edges on the InN content differs from that for the virtual crystal approximation. The energy positions of the conduction and valence band edges of GaN relative to the InAlN band gap is also presented, provided that $\Delta E_C^{AlN/GaN}$ = 1.85 (~1.8) eV, $\Delta E_C^{GaN/InN}$ = 2.19 (~1.9) eV, and $\Delta E_C^{AlN/InN}$ = 3.9 (~3.7) eV and, correspondingly, $\Delta E_V^{AlN/GaN}$ = 0.9 (~1.0) eV, $\Delta E_V^{GaN/InN}$ = 0.62 (~0.8) eV, and $\Delta E_V^{AlN/InN}$ = 1.5 (~1.8) eV.

The discontinuities of the corresponding bands without taking into account elastic stresses and the presence of a polarizing surface charge at the interface are taken from [53]. In parentheses, similar estimates of the energy-band discontinuities obtained on the basis of the calculated values of the CNL level position in these compounds under the same assumptions are presented. Experimental values obtained from X-ray photoelectron spectroscopy give $\Delta E_V^{AlN/InN}$ = (1.52 ± 0.17) eV and $\Delta E_C^{AlN/InN}$ = (4.0 ± 0.3) eV [54]. Experimental data for InN/GaN give $\Delta E_V^{GaN/InN}$ = 0.8 eV and $\Delta E_C^{GaN/InN}$ = 1.9 eV for the (0001) planes and $\Delta E_V^{GaN/InN}$ = 1.2 eV and $\Delta E_C^{GaN/InN}$ = 1.5 eV for the (000-1) planes [55].

Figure 3 shows the energy position of the CNL level in InAlN relative to its conduction and valence band edges as a function of the solution composition. The given dependences show that at x <0.4, the CNL level in the InAlN solid solution is located in the upper half of the band gap, and for x> 0.4, it falls into the region of allowed energies of the conduction band, as is the case for InN [56]. Given the presence of an AlN spacer layer (d = 1–1.5 nm) for the LM-InAlN/AlN/GaN structure, the estimated values are $\Delta E_C^{InAlaN/AlN} \approx$ 1.2 eV and $\Delta E_V^{InAlaN/AlN} \approx$ 0.5 eV for the band gap of the barrier layer $E_g \approx$ 4.5 eV. In undoped LM - InAlN layers, the electron concentration due to residual donors is ~(1–8)·10^{18} cm^{-3} [48–50] and the CNL level position is ≈E_C – 1.6 eV. This provides high rate of removal of free electrons in the InAlN barrier layer under irradiation. In this case, for x> 0.44, both the initial and irradiated InAlN samples are degenerate n^+-type materials. In turn, the AlGaN layers will have a low value of $-\Delta n/\Delta D$, since the initial free electron density in them is low and decreases with increasing Al content. This is even truer for the AlN-based barrier layer. These estimates are generally confirmed by numerous experimental measurements of the free electron removal rates under irradiation of the corresponding HEMT structures [5, 40, 43].

CONCLUSIONS

As a result of studies, it was shown that radiation traps, mainly acceptor-type traps, which reduce the electron mobility and density of a two-dimensional electron gas in the conducting channel and also increase the trapping effect of these electrons in the dynamic measurements, are responsible for the changes in the parameters of irradiated HEMT structures. Irradiation with protons, electrons, gamma rays, or neutrons reveals common features of degradation of static and dynamic parameters of InAlN/GaN и AlGaN/GaN heterostructures. These features include an increase in the contact and layer specific resistivity, in the dynamic resistance of the structure in the on-state, in the reverse gate leakage current, the breakdown voltage, and critical voltage, as well as a decrease in the static drain current and steepness of the current-voltage characteristic, in the cut-off and maximum frequencies, an increase in the current collapse, a negative shift of the threshold voltage at a low density of radiation defects and, accordingly, a positive shift with increasing radiation dose. The main reason for the electron mobility degradation upon irradiation is an increase in the interface roughness. The carrier removal rates in InAlN/GaN and AGaN/GaN HEMTs upon irradiation are determined primarily by the initial electronic properties of the corresponding barrier layers and by the CNL level position in these semiconductors, namely, by high free electron density in the InAlN layers and, accordingly, their low density in AlGaN layers and especially in AlN.

This work was financially supported by the Project “Research and development of the manufacturing technology of ultra-high-frequency monolithic integrated circuits based on InAlN/GaN heterostructures for space applications” No. 14.578.21.0240 (agreement 26.09. 2017), Unique Identifier of the Project RFMEFI 57817X240.

REFERENCES

1. A. Ionascut-Nedelcescu, C. Carlone, A. Houdayer, *et al*., IEEE Trans. Nucl. Sci., **49(6)**, 2733 (2002).
2. D. C. Look, D. C. Reynolds, J. H. Hemsky, *et al*., Phys. Rev. Lett., **79(12)**, 2273 (1997).
3. J. Nord, K. Nordlund, J. Keinonen, *et al*., Nucl. Instrum. Methods Phys. Res. B, **202**, 93 (2003).
4. H. Y. Xiao, F. Gao, X. T. Zu, and W. J. Weber, J. Appl. Phys., **105**, 123527 (2009).
5. S. J. Pearton, Y.-H. Hwang, and F. Ren, ECS Transactions, **66(1)**, 3 (2015).
6. J. F. Ziegler, J. P. Biersack, and U. Littmark, The Stopping and Range of Ions in Solids, Pergamon Press, London (1996).
7. J. F. Ziegler, SRIM, The Stopping and Range of Ions in Matter, Electronic resource, URL: http://www.srim.org (10.06.2019).
8. V. N. Brudnyi, N. G. Kolin, and L. S. Smirnov, Semiconductors, **41(9)**, 1011 (2007).
9. V. N. Brudnyi, S. N. Grinyaev, and N. G. Kolin, Semiconductors, **37(5)**, 537 (2003).
10. V. N. Brudnyi, A. V. Kosobutskii, and N. G. Kolin, Russ. Phys. J., **51**, No. 12, 1270 (2008).
11. V. N. Brudnyi, A. V. Kosobutskii, and N. G. Kolin, Semiconductors, **43(10)**, 1271 (2009).
12. V. N. Brudnyi, V. M. Boiko, N. G. Kolin, *et al*., Semicond. Sci. Technol., **33**, 095011 (2018).
13. A. Castaldini, A. Cavallini, L. Polenta, *et al*., J. Phys. Condens. Matter., **12**, 10161 (2000).
14. F. D. Auret, S. A. Goodman, F. K. Koschnick, *et al*., Appl. Phys. Lett., **74**, 407 (1999).
15. F. D. Auret, S. A. Goodman, F. K. Koschnick, *et al*., Appl. Phys. Lett., **73**, 3745 (1998.
16. A. Ya. Polyakov, A. S. Usikov, B. Theys, *et al*., Solid-State Electron., **44**, 1971 (2000).
17. S. J. Pearton and A.Ya. Polyakov, Int. J. Mater. Structural Integrity., **2**, 93 (2008).
18. K. C. Collins, A. M. Armstrong, A. A. Allerman, *et al*., J. Appl. Phys., **122**, 235705 (2017).
19. Z. Zhang, E. Farzana, W. Y. Sun, *et al*., J. Appl. Phys., **118**, 155701 (2015).
20. P. N. M. Ngoepe, W. E. Meyer, and F. D. Auret, Mater. Sci. Semicond. Process., **64**, 29 (2017).
21. Z. Zhang, A. R. Arehart, E. Cinkilic, *et al*., Appl. Phys. Lett., **103**, 042102 (2013).
22. S. A. Goodman, F. D. Auret, M. J. Legodi, *et al*., Appl. Phys. Lett., **78**, 3815 (2001).
23. N. M. Shmidt, D. V. Davydov, V. V. Emtsev, *et al*., Phys. Stat. Sol. (b), **216**, 533 (1999).
24. Z.-Q. Fang, J. W. Hemsky, D. C. Look, *et al*., Appl. Phys. Lett., **72**, 448 (1998).
25. L. Polenta, Z.-Q. Fang, and D. C. Look, Appl. Phys. Lett., **76**, 2086 (2000).

26. C.-W. Wang, B.-S. Soong, J.-Y. Chen, *et al*., J. Appl. Phys., **88**, 6355 (2000).
27. A.Ya. Polyakov, In-Hwan Lee, N. B. Smirnov, *et al*., J. Appl. Phys., **109**, 123703 (2011).
28. Duc Tran Thien, Pozina Galia, Son Nguyen Tien, *et al*., J. Appl. Phys., **119**, 095707 (2016).
29. P. N. M. Ngoepe, W. E. Meyer, F. D. Auret, *et al*., Physica B, **535**, 96 (2018).
30. S. A. Goodman, F. D. Auret, G. Myburg, *et al*., Mater. Sci. Eng. B, **82**, 95 (2001).
31. I-H. Lee, A. Y. Polyakov, E. B. Yakimov, *et al*., Appl. Phys. Lett., **110**, 112102 (2017).
32. V. N. Brudnyi, S. S. Verevkin, A. V. Govorkov, *et al*., Semiconductors, **46(4)**, 433 (2012).
33. J. Kuzmik, IEEE Electron Device Lett., **22(11)**, 510 (2001).
34. I. Rossetto, F. Rampazzo, *et al*., Proc. of 44-th European Sol. State Device Research Conf. (ESSDERC), Venice, Italy (2014).
35. I. Rossetto, F. Rampazzo, S. Gerardin, *et al*., Sol.-State Electron., **113**, 15 (2015).
36. C.-F. Lo, L. Liu, F. Ren, *et al*., J. Vac. Sci. Technol. B, **30(4)**, 041206 (2012).
37. H.-Y. Kim, C. F. Lo, L. Liu, *et al*., Appl. Phys. Lett., **100**, 2107 (2012).
38. C.-F. Lo, L. Liu, F. Ren, *et al*., J. Vac. Sci. Technol. B, **29(6)**, 061201 (2011).
39. C.-F. Lo, L. Liu, T. S. Kang, *et al*., J. Vac. Sci. Technol. B, **30(3)**, 031202 (2012).
40. S. Ahn, B.-J. Kim, Y.-H. Lin, and F. Ren, J. Vac. Sci. Technol. B, **43(5)**, 051202 (2016).
41. T. Anderson, A. Koehler, Y.-H. Hwang, *et al*., J. Vac. Sci. Technol. B, **32(5)**, 051203 (2014).
42. Y.-S. Hwang, L. Liu, F. Ren, *et al*., J. Vac. Sci. Technol. B, **31(2)**, 022206 (2013).
43. H.-Y. Kim, J. Kim, L. Liu, *et al*., J. Vac. Sci. Technol. B, **31(5)**, 051210 (2013).
44. M. D. Smith, D. O'Mahony, F. Vitobello, *et al*., Semicond. Sci. Technol., **31**, 025008 (2016).
45. M. D. Smith, Development of InAlN HEMTs for space application: PhD Thesis, University College Cork, Ireland (2016).
46. A.Ya. Polyakov, N. B. Smirnov, A. V. Govorkov, *et al*., J. Vac. Sci. Technol. B, **30(6)**, 061207 (2012).
47. N. Dawahre and C. Shen, J. Vac. Sci. Technol. B, **31**, 041802 (2013).
48. R. Butte, J-F. Carlin, E. Feltin, *et al*., J. Phys. D: Appl. Phys., **40**, 6328 (2007).
49. Y. Taniyasu, J.-F. Carlin, A. Castiglia, *et al*., Appl. Phys. Lett., **101**, 082113 (2012).
50. M. Goncshorek, J.-F. Carlin, E. Feltin, *et al*., J. Appl. Phys., **103**, 093714 (2008).
51. S. Yamaguchi, M. Kariya, S. Nitta, *et al*., Appl. Phys. Lett., **76(7)**, 876 (2000).
52. J. Li, K. B. Nam, J. Y. Lin, and H. X. Jiang, Appl. Phys. Lett., **79(20)**, 3245 (2001).
53. S. Schulz, M. A. Caro, L.-T. Tan, *et al*., Appl. Phys. Express., **6(12)**, 1 (2013).
54. D. C. King, T. D. Veal, P. H. Jefferson, *et al*., Appl. Phys. Lett., **90**, 132105 (2007).
55. S.-C. Lin, C.-T. Kim, X. Liu, *et al*., Appl. Phys. Express., **5**, 031003 (2012).
56. S. X. Li, K. M. Yu, R. E. Jones, *et al*., Phys. Rev. B, **71**, 161201(R) (2005).